



Melatonin attenuates AFB1-induced cardiotoxicity via the NLRP3 signalling pathway

Hui Yan^{1,*}, Junhua Ge^{2,*} , Hongrui Gao¹,
Yang Pan¹, Yan Hao¹ and Jian Li² 

Abstract

Objective: This study was conducted to investigate the protective effect of melatonin against aflatoxin B1 (AFB1) cardiotoxicity by evaluating NOD-like receptor family pyrin domain containing protein 3 (NLRP3) signalling.

Methods: Four groups of five rats each were assessed: control group (vehicle only), two AFB1 (0.15 and 0.3 mg/kg)-treated groups, and a combined AFB1 (0.3 mg/kg) plus melatonin (5 mg/kg)-treated group. After 6 weeks of once-daily intragastric treatment, cardiac pathologic changes were observed under optical microscopy, and oxidative/antioxidative parameters were measured in myocardial homogenate. Cardiac tissue expression of *NLRP3* and other important inflammatory components was also analysed.

Results: Compared with controls, increasing concentrations of AFB1 were associated with increased oxidative stress and caused myocardial structure damage. In addition, AFB1 dose-dependently activated the NLRP3 signalling pathway. All these indices were significantly ameliorated by combined AFB1 plus melatonin treatment versus high-dose AFB1 alone.

Conclusion: Melatonin may reduce NLRP3 inflammasome activation by inhibiting oxidative stress and thus protect against injury from AFB1-induced myocardial toxicity.

Keywords

Aflatoxin B1, oxidative stress, NLRP3 inflammasome, melatonin, myocardial toxicity

Date received: 21 January 2020; accepted: 30 July 2020

¹Department of Cardiology, College of Medical Sciences, Qingdao University, Shandong, China

²Department of Cardiology, The Affiliated Hospital of Qingdao University, Shandong, China

*These authors contributed equally to this work

Corresponding author:

Jian Li, Department of Cardiology, The Affiliated Hospital of Qingdao University, 16 Jiangsu Road, Qingdao 266000, Shandong Province, China.

Email: leerabbity@126.com

Introduction

Aflatoxins are a group of mycotoxins derived from *Aspergillus flavus* and *Aspergillus parasiticus*.¹ Among the



Creative Commons Non Commercial CC BY-NC: This article is distributed under the terms of the Creative

Commons Attribution-NonCommercial 4.0 License (<https://creativecommons.org/licenses/by-nc/4.0/>) which permits non-commercial use, reproduction and distribution of the work without further permission provided the original work is attributed as specified on the SAGE and Open Access pages (<https://us.sagepub.com/en-us/nam/open-access-at-sage>).

aflatoxins, aflatoxin B1 (AFB1) seems to be the most hazardous to health and has been extensively studied for its hepatotoxicity.² Although the main target of AFB1 toxicity is the liver, AFB1 is also indicated to exert harmful effects on other organs, including the heart.^{3,4} Oxidative stress is one manifestation of AFB1-induced cardiotoxicity, and antioxidant therapy is associated with significantly reduced AFB1-induced myocardial damage in rats.⁴

Various external stresses, including oxidative stress, are now known to activate the NOD-like receptor family pyrin domain-containing protein 3 (NLRP3) inflammasome.⁵ The NLRP3 inflammasome is a polyprotein complex consisting of NLRP3, apoptotic spot-like protein containing a caspase activation and recruitment domain (CARD; known as ASC), and procaspase-1. As the first step in NLRP3 inflammasome activation, caspase-1 is automatically cleaved into active forms (p20 subunits) that are responsible for programmed cell death and the secretion of inflammatory markers, including interleukin (IL)-1 β and IL-18, thereby augmenting the inflammatory cascade and aggravating tissue injury.^{6,7} The NLRP3 inflammasome has been found to be activated in every heart cell type under appropriate stimulation conditions.⁸ However, the role of NLRP3 in myocardial damage induced by AFB1 remains unclear. Recently, AFB1 was found to activate the NLRP3 inflammasome in primary hepatocytes and Kupffer cells, leading to liver inflammatory injury.⁹ It seems reasonable that a similar activation method may be induced by AFB1 in the heart.

Melatonin (n-acetyl-5-methoxytryptamine), a neuroendocrine hormone secreted mainly by the pineal gland, is also a very effective antioxidant,¹⁰ and its early administration significantly attenuates AFB1-induced tissue injury.¹¹ Melatonin can easily enter cellular and subcellular compartments, advantageously outperforming

other antioxidants in the attenuation of oxidative stress.¹² Apart from its direct scavenging effect on free radicals, melatonin also reportedly functions as an antioxidant via other methods, such as by stimulating antioxidant enzymes while suppressing the activity of pro-oxidant enzymes.¹³ Melatonin's ability to inhibit activation of the NLRP3 inflammasome, due to its various antioxidant actions, has been fully documented in many experimental studies.¹⁴⁻¹⁶

The purpose of the present study was to determine levels of oxidative stress in heart homogenates of rats treated with AFB1, and to study the correlation between oxidative stress and NLRP3 inflammasome activation. In addition, the antioxidant melatonin was investigated regarding whether it protects against AFB1-induced myocardial damage by regulating the NLRP3 signalling pathway.

Materials and methods

Study animals

The experimental protocol was approved by the Animal Care and Welfare Committee of the Affiliated Hospital of Qingdao University (reference no: AHQU-MAL2018079), and all procedures were performed according to guidelines established by the Care and Use of Laboratory Animals published by the Ministry of Science and Technology of China. Twenty male Sprague-Dawley rats (age 8 weeks; weight range, 250–280 g) were provided by Beijing Vital River Laboratory Animal Technology Inc. (Beijing, China). All rats were housed in a specific pathogen-free room (25°C and 65% humidity) and exposed to a 12-h light/12-h dark cycle; the rats were fed a standard laboratory diet and had free access to water. After acclimatization for 1 week, the rats were randomly divided into four groups (five

animals/group) and administered treatments by gastric intubation daily for 6 weeks as follows:

Group I: Control group, treated with vehicle only (0.5% dimethyl sulphoxide [DMSO]/ physiological saline, and 2.5% ethanol/ physiological saline).

Groups II and III: Treated with 0.15 and 0.3 mg/kg AFB1, respectively, dissolved in 0.5% DMSO/ physiological saline.

Group IV: Treated with 0.3 mg/kg AFB1 dissolved in 0.5% DMSO/ physiological saline plus 5 mg/kg melatonin, dissolved in 2.5% ethanol/ physiological saline.

Melatonin (Sigma-Aldrich, St Louis, MO, USA) was administered 2 h before sunset, and AFB1 (Chengzhu Biotechnology Co. Ltd., Shanghai, China) was administered 30 min following melatonin. At 24 h following the last administration, rats were anaesthetized using 40 mg/kg pentobarbital sodium (i.p.), and arterial blood was rapidly collected. The rat hearts were also collected for follow-up experiments.

Determination of LDH levels

Lactate dehydrogenase (LDH) was measured as an indirect indicator of tissue damage. Briefly, blood samples were collected from the abdominal aortas of all rats and immediately centrifuged at 3000 × *g* for 20 min to prepare serum. Serum LDH levels were then measured using an LDH assay kit (Jiancheng Bioengineering Institute, Nanjing, China) according to the manufacturer's protocol.

Histological examination

The hearts were collected from all rats for analysis. A 5 mm × 5 mm piece of cardiac tissue was taken from the left ventricular

region, fixed using 4% neutral paraformaldehyde, then embedded in paraffin wax using a standard protocol. Next, 4-μm thick sections were cut and mounted onto glass slides for haematoxylin and eosin (H&E) staining and immunohistochemistry, as described below. The sections were subsequently observed at 200 × magnification, using an optical microscope (Olympus, Tokyo, Japan). For each sample, five random fields were observed. The resulting images were analysed in a blind manner.

Morphometrical analysis of H&E stained sections was performed as follows. The cardiomyocyte degeneration, including myocardial oedema and muscle fibre degeneration, was quantified using a 0 to 4-point scale:¹⁷ 0, no injury; 1, lesion range < 25%; 2, lesion range 25–49%; 3, lesion range 50–75%; and 4, lesion range > 75%. In addition, the degree (score 0–3) of inflammatory cell infiltration was analysed according to a previously described scoring method:¹⁸ 0, none; 1, mild; 2, moderate; or 3, severe.

Sections were analysed by immunohistochemistry, as described previously.¹⁹ After routine dewaxing and rehydration, heart sections were subjected to antigen retrieval using citrate buffer (pH 6.0), followed by treatment with 3% hydrogen peroxide for 10 min at room temperature to block endogenous peroxidase. Nonspecific binding in tissue samples was blocked by incubation with goat serum at room temperature for 20 min, then sections were incubated with rabbit anti-rat nuclear factor (NF)-κB (1:250 dilution; Cell Signalling Technology, Danvers, MA, USA) and rabbit anti-rat NLRP3 (1:100 dilution Abcam, Millbrae, CA, USA) primary antibodies for 1 h at 37 °C. Sections were then washed in phosphate buffered saline (PBS) three times, and exposed to biotinylated anti-rabbit IgG secondary antibody (Zhongshan Golden Bridge Biological Co., Beijing, China) for 30 min at 37 °C.

Sections not exposed to primary antibody served as negative controls. Positive immunoreactivity was visualized as brown or yellow staining using 3,3-diaminobenzidine (DAB). The level of immunostaining was semi-quantified using Image-Pro Plus (IPP) software, version 6.0 (Media Cybernetics, Inc., Rockville, MD, USA). NLRP3 reactivity was scored according to the level of staining intensity (0, none; 1, light yellow; 2, yellow-brown; or 3, brown). For NF- κ B protein, positive immunostaining was defined as the presence of brown or yellow granules in the nucleus. Positively stained cells and total cells under each field were counted, and the reactivity was evaluated as the proportion of positively-stained cells.

Determination of oxidative stress and antioxidant enzyme levels

Portions of fresh rat myocardium were harvested and used to prepare a 10% homogenate, which was centrifuged at $1\,000 \times g$ for 10 min at 4°C . The supernatant was then collected for subsequent analyses of oxidative stress markers using relevant assay kits (all Beyotime Biotechnology, Shanghai, China), according to the manufacturer's protocols. The concentration of malondialdehyde (MDA) was assessed using the thiobarbituric acid reaction kit, and superoxide dismutase (SOD) activity was measured using the water-soluble tetrazolium salt (WST)-8 kit. Generation of reactive oxygen species (ROS) was estimated with the fluorescent probe 2,7-dichlorodihydrofluorescein diacetate (DCFHDA), as previously described.^{20,21} For each sample, levels of ROS were expressed in terms of DCF fluorescence generation/ mg protein/ min.

Western blotting and immunoprecipitation

Protein was extracted from frozen cardiac tissue using RIPA lysis buffer containing a proteinase inhibitor cocktail (1:100 dilution, Sigma-Aldrich), and protein concentration was determined using a BCA assay kit (Solarbio Scientific Co., Ltd, Beijing, China), following the manufacturer's instructions. Total protein was separated by 10–12.5% sodium dodecyl sulphate-polyacrylamide gel electrophoresis (SDS-PAGE) and transferred onto 0.22- μm polyvinylidene fluoride (PVDF) membranes. The membranes were blocked in 5% non-fat milk for 2 h at room temperature and incubated with the following primary antibodies at 4°C overnight: anti- β -actin (internal control, 1:10 000 dilution), anti-p65 (1:1 000 dilution), and anti-phosphorylated p65 (1:1 000 dilution) (all Cell Signalling Technology); anti-NLRP3 (1:800 dilution), anti-caspase-1 (1:200 dilution), and anti-IL-1 β (1:1 000 dilution) (all Abcam); and anti-ASC (1:300 dilution; Santa Cruz Biotechnology, Dallas, TX, USA). Membranes were then washed three times with 0.1% Tween-20/Tris-buffered saline (TBS) for 5 min each and incubated with the corresponding HRP-conjugated secondary antibodies at room temperature for 1 h: goat anti-rabbit IgG (1:5 000 dilution) and goat anti-mouse IgG (1:5 000 dilution) (both Elabscience Biotechnology, Wuhan, China). An enhanced chemiluminescence reagent (Merck Millipore, Billerica, MA, USA) was added to visualize the protein signal, and greyscale values were analysed using ImageJ software, version 1.8.0 (NIH, Bethesda, MD, USA).

The interaction between NLRP3 and ASC was analysed by immunoprecipitation.²² Proteins were first extracted with RIPA lysis buffer (as above), and protein concentration adjusted to 1 $\mu\text{g}/\text{ul}$ with PBS. For each sample, one part of the

diluted solution was used directly for Western blots with anti-NLRP3 primary antibody (positive control), and the other part (100 μ g) was incubated with an anti-ASC antibody in an immunoprecipitation buffer for 12 h at 4°C with gentle rotation followed by treatment with protein A-sepharose beads (50 μ l) for another 12 h. The beads were then washed and resuspended, followed by Western blotting with anti-NLRP3 and -ASC antibodies. The density of these two protein bands was then measured using Image J software, version 1.8.0, and the relative level was calculated by the following formula: density value of the NLRP3 band / density value of the ASC band.

Statistical analyses

Statistical analyses were performed using SPSS software, version 19.0 (SPSS Inc., Chicago, IL, USA), and results are presented as mean \pm SD or mean \pm SEM. Measurement data were analysed by one-way analysis of variance followed by a post hoc test (Holm-Sidak). Associations between two variables were determined using Pearson's correlation analysis. A multiple linear regression model was constructed to analyse the association of ROS levels with cardiovascular damage index and protein expression levels. A P -value <0.05 was considered to indicate statistical significance.

Results

Changes in biochemical and cardiac histological characteristics in rats

Biochemical analyses showed that serum LDH levels in response to AFB1 treatment were increased versus vehicle alone (control), but the increased LDH was only statistically significant versus controls in the 0.3 mg/kg AFB1 group ($P <0.001$).

Supplementation with 5 mg/kg melatonin significantly attenuated the increase in LDH caused by 0.3 mg/kg AFB1 ($P <0.01$; Figure 1a). The cardiotoxicity of AFB1 was further evaluated from a morphological perspective, mainly with H&E staining. Both low (0.15 mg/kg) and high (0.3 mg/kg) concentrations of AFB1 led to cardiac pathologic injury, with greater cardiomyocyte degeneration and inflammatory cell infiltration in the AFB1 groups compared with controls, particularly in the high-dose group. The changes induced by 0.3 mg/kg AFB1 were significantly reduced following coadministration of 5 mg/kg melatonin (all $P <0.05$; Figure 1b and c).

Melatonin attenuates the oxidative stress response caused by AFB1

Melatonin inhibited the adverse effects of AFB1 on antioxidant levels and exhibited a protective effect (Figure 2). ROS levels in the heart increased with increasing concentrations of AFB1 compared with vehicle alone ($P <0.05$), and ROS levels were significantly attenuated with melatonin treatment ($P <0.01$, Figure 2a). In addition, 0.3 mg/kg AFB1 significantly inhibited SOD activity, and the inhibitory effect was significantly reversed by melatonin (both $P <0.05$; Figure 2b). Supplementation with melatonin significantly inhibited the increase in MDA concentration induced by 0.3 mg/kg AFB1 (all $P <0.01$; Figure 2c). In addition, the degree of cardiomyocyte degeneration was found to positively correlate with ROS levels in response to treatment with AFB1 ($r = 0.71$, Figure 2d).

Levels of NLRP3 in myocardial tissue

Levels of heart tissue NLRP3 were analysed by immunohistochemistry. Semi-quantitative evaluation showed a numerical increase in heart tissue NLRP3 expression

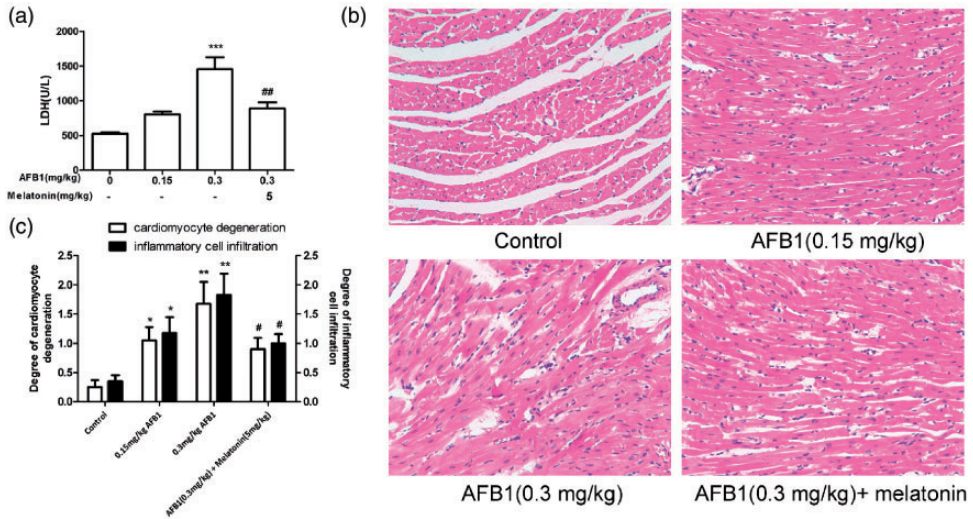


Figure 1. Changes in biological characteristics and cardiac histology in rats treated with aflatoxin B1 (AFB1): (a) serum lactate dehydrogenase (LDH) concentrations; (b) representative images of haematoxylin and eosin stained sections showing cardiac pathologic injury in response to 0.15 and 0.3 mg/kg AFB1, characterized by cardiomyocyte degeneration, pink proteinaceous mucus exudation and inflammatory cell infiltration. Tissue damage remained following melatonin treatment, but inflammatory cell infiltration was visibly alleviated, with little exudation of pink proteinaceous mucus in the cardiac interstitium (original magnification, $\times 200$); and (c) quantification of the degree of cardiomyocyte degeneration and inflammatory cell infiltration in each group. Data presented as mean \pm SEM. * $P < 0.05$, ** $P < 0.01$, and *** $P < 0.001$ versus controls; # $P < 0.05$, and ## $P < 0.01$ versus the 0.3 mg/kg AFB1 group.

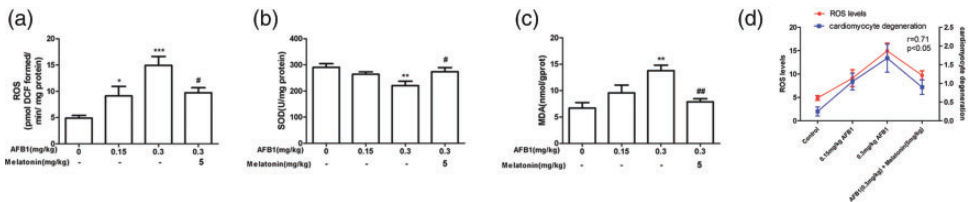


Figure 2. Melatonin attenuates the oxidative stress response caused by aflatoxin B1 (AFB1): (a) reactive oxygen species (ROS) generation; (b) superoxide dismutase (SOD) activity and (c) malonaldehyde (MDA) concentrations in myocardial homogenates; (d) correlation between ROS levels and the degree of cardiomyocyte degeneration ($r = 0.71$, $P < 0.05$). Data presented as mean \pm SEM. * $P < 0.05$, ** $P < 0.01$, and *** $P < 0.001$ versus controls; # $P < 0.05$ and ## $P < 0.01$ versus the 0.3 mg/kg AFB1 group.

in response to both AFB1 doses (0.15 and 0.3 mg/kg), however, the increase was only statistically significant in the high-dose AFB1 treatment group compared with controls ($P < 0.01$). Melatonin significantly

attenuated the AFB1-induced *NLRP3* expression ($P < 0.001$ versus 0.3 mg/kg AFB1; Figure 3a and b). Similar results were found by Western blot analysis ($P < 0.05$, Figure 3c and d).

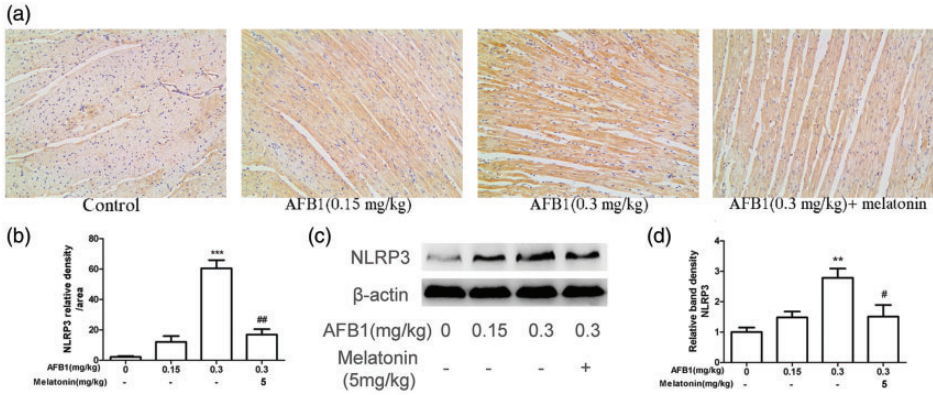


Figure 3. NOD-like receptor family pyrin domain-containing protein 3 (NLRP3) levels in myocardial tissue of rats treated with 0.15 and 0.3 mg/kg aflatoxin B1 (AFB1) or 0.3 mg/kg AFB1 plus 5 mg/kg melatonin: (a) representative images of immunohistochemical NLRP3 staining in myocardial tissues (original magnification, $\times 200$); (b) semi-quantification of NLRP3 expression in each group; (c) representative Western blots of NLRP3 expression in myocardial tissues in the different groups; and (d) relative quantification of NLRP3 levels using GAPDH as reference. Data presented as mean \pm SD. $**P < 0.01$ and $***P < 0.001$ versus controls; $\#P < 0.05$ and $###P < 0.01$ versus 0.3 mg/kg AFB1 group.

Melatonin prevents activation of NLRP3 in myocardial tissue exposed to AFB1

Expression of other proteins involved in inflammasome formation was also assessed by Western blot analysis (Figure 4a and b). The hearts of rats exposed to AFB1 had significantly higher levels of ASC expression in the group exposed to 0.3 mg/kg AFB1 versus controls ($P < 0.01$), and levels of caspase-1p20 and IL-1 β p17, which serve as indicators of NLRP3 activation, were significantly increased with both AFB1 doses ($P < 0.05$ versus controls). Furthermore, correlation analysis in the AFB1 groups showed that ROS levels were positively correlated with NLRP3 ($r = 0.79$, Figure 4c), ASC ($r = 0.75$, Figure 4d), caspase-1p20 ($r = 0.86$, Figure 4e) and IL-1 β p17 expression ($r = 0.74$, Figure 4f). Compared with levels in the high-dose AFB1 group, levels of ASC, caspase-1p20 and IL-1 β p17 were significantly decreased in the melatonin coadministration group ($P < 0.05$). Evaluation of the interaction between NLRP3 and ASC by co-immunoprecipitation demonstrated that

AFB1 dose-dependently induced NLRP3 inflammasome formation, as shown by the increased interaction of NLRP3 with ASC in heart tissue with increasing AFB1 concentration (Figure 4g and h). Melatonin significantly reduced the interactions between NLRP3 and ASC, suggesting that it inhibited inflammasome assembly ($P < 0.05$, Figure 4g and h).

Effects of melatonin on NF- κ B pathway activation in myocardial tissue

Major regulatory proteins involved in the NF- κ B pathway were assessed via proteomic analyses using Western blots. Initial analysis of NF- κ B phosphorylation showed that, compared with vehicle alone, AFB1 significantly upregulated the p-p65/p65 ratio in a dose-dependent manner, and melatonin pretreatment significantly reduced the phosphorylation of NF- κ B stimulated by high-dose AFB1 ($P < 0.05$, Figure 5a and b). To further verify these results, the intracellular localization of p65 was assessed by immunohistochemistry. AFB1 was found to increase the proportion

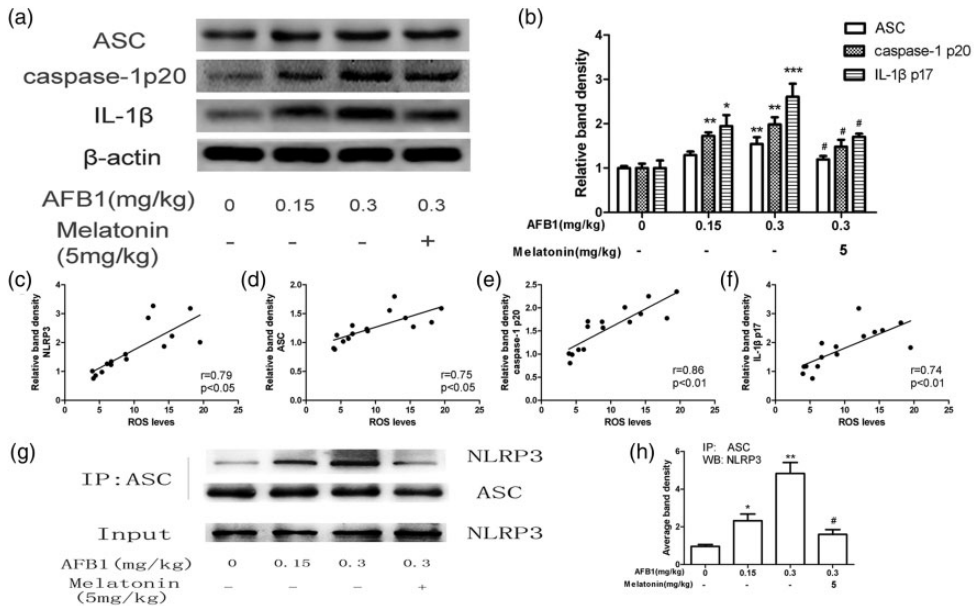


Figure 4. Melatonin prevents activation of NOD-like receptor family pyrin domain-containing protein 3 (NLRP3) in myocardial tissue exposed to aflatoxin B1 (AFB1): (a) representative Western blot showing changes in expression of apoptosis-associated speck-like protein containing a CARD (ASC; upper panel), *Caspase-1p20* (middle panel) and interleukin (IL)-1 β p17 (bottom panel) in each group; (b) relative quantification of ASC, *Caspase-1p20* and *IL-1 β p17* expression; (c-f) correlations between reactive oxygen species (ROS) levels and (c) NLRP3, (d) ASC, (e) caspase-1p20, and (f) IL-1 β p17 levels; (g) representative Western blot showing NLRP3 levels (upper panel) and ASC levels (middle panel) in sample lysates that underwent immunoprecipitation with ASC, and NLRP3 levels (bottom panel) in sample lysates that did not undergo immunoprecipitation; and (h) quantification of interactions between myocardial NLRP3 and ASC in the different groups. Data presented as mean \pm SEM. * $P < 0.05$, ** $P < 0.01$, and *** $P < 0.001$ versus controls; # $P < 0.05$ versus 0.3 mg/kg AFB1 group.

of NF- κ B-positive cells, particularly in the high-dose group, in which it was 10.4-fold higher than controls. Moreover, the ratio was significantly lower in the melatonin intervention group versus the high-dose AFB1 group ($P < 0.001$; Figure 5c and d). The p-p65/p65 ratio in the AFB1 groups was also shown to be correlated with ROS levels ($r = 0.82$; Figure 5e) and *NLRP3* expression ($r = 0.86$; Figure 5f).

Discussion

Exposure to xenobiotics is implicated in the development of multiple heart diseases,

including viral myocarditis and alcoholic cardiomyopathy.^{23,24} Aflatoxin B1 (AFB1), a carcinogenic mycotoxin widely found in mildewed cereals, is absorbed and rapidly distributed to the heart. Studies have shown that AFB1 disrupts mitochondrial function and leads to the release of ROS resulting in cardiomyocyte damage, which is the main reason for the cardiotoxicity of AFB1.²⁵ Consistent with this evidence, the present study revealed that AFB1 induces oxidative stress in the rat myocardium, and AFB1 promotes NLRP3 inflammasome activation through a ROS-dependent pathway. In addition,

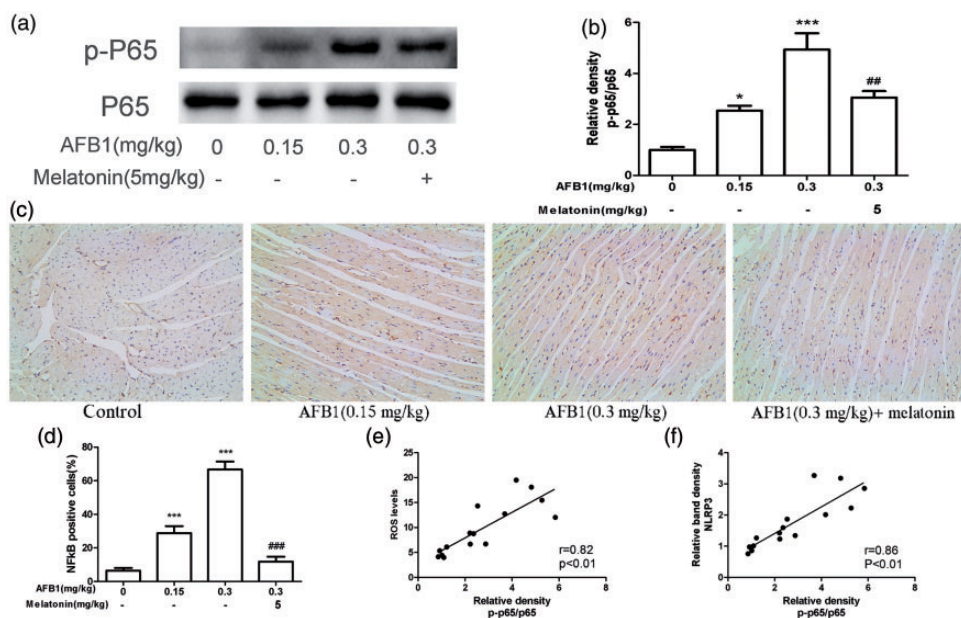


Figure 5. Effects of aflatoxin B1 (AFB1) and melatonin on nuclear factor (NF)- κ B pathway activation in rat myocardial tissue: (a) representative Western blots showing levels of p-p65 and p65 in myocardial tissues; (b) quantitative analysis of the p-p65/p65 ratio in different treatment groups (the mean value for the control group was standardized to 1.0); (c) representative immunohistochemistry images for evaluation of nuclear NF- κ B-positive cells in myocardial tissues (original magnification, $\times 200$); (d) quantitative analysis of nuclear NF- κ B positivity under different treatments; (e and f) correlations between p-p65/p65 ratio and (e) cardiac reactive oxygen species (ROS) levels; and (f) NOD-like receptor family pyrin domain-containing protein 3 (NLRP3) expression. Data presented as mean \pm SD. * $P < 0.05$ and *** $P < 0.001$ versus controls; ## $P < 0.01$ and ### $P < 0.001$ versus 0.3 mg/kg AFB1 group.

melatonin was found to exert a beneficial effect on AFB1-induced cardiac injury that might be related to the alleviation of oxidative stress and therefore the inhibition of NLRP3 inflammasome activation.

Activation of the NLRP3 inflammasome was conventionally considered to be a protective response. For example, the activated NLRP3 inflammasome in invasive pulmonary aspergillosis has been shown to function to control infection,²⁶ and the NLRP3 inflammasome and subsequent production of IL-18 protect mice from death during experimental infection with *P. brasiliensis*.²⁷ These findings demonstrate that the NLRP3 inflammasome plays important roles in innate antifungal immunity,

however, other studies have found that overactivation of the NLRP3 inflammasome may lead to further damage. *Candida albicans* cell wall extracts induced endothelial cell pyroptosis by activating caspase-1, whereas addition of the NLRP3 inhibitor MCC950 significantly alleviated pyroptotic endothelial cell death.²⁸ Zhang et al.⁹ reported that the severity of AFB1-induced liver inflammatory injury in mice was significantly alleviated by downregulating NLRP3 expression through inhibition of cyclooxygenase-2. These results imply that persistent activation of the NLRP3 inflammasome is a critical factor for instigating tissue damage. Here, the role of NLRP3 in myocardial injury was

investigated by infecting rats with AFB1. The present data revealed that AFB1 elicited activation of the NLRP3 inflammasome in a dose-dependent manner, which in turn triggered the secretion of mature IL-1 β and the release of LDH; therefore, NLRP3 inflammasome activation might be an important mechanism underlying the cardiac damage caused by AFB1. The present study suggests that cardiac damage and inflammation are consequences of not only the direct toxic effect of AFB1, but also indirect toxic injury mediated by NLRP3 inflammasome hyperactivation.

The NLRP3 inflammasome is composed of NLRP3, ASC and procaspase-1,²⁹ and its activation in the heart is known to occur in two independent steps:^{30,31} the expression of pyroptosis protein markers (e.g., NLRP3 and pro-IL-1 β), which is followed by the activation of NLRP3 and the formation of inflammasomes responsible for programmed cell death, and the secretion of inflammatory markers, such as IL-1 β and IL-18. Several signals, including K⁺ efflux, ROS overproduction and lysosome rupture, have been recognized to activate the NLRP3 inflammasome.⁸ The present results showed that heart tissue ROS levels were increased in AFB1-treated rats, as was the degree of cardiac injury; furthermore, these changes were revealed to be interrelated. The present findings are consistent with the notion that oxidative stress plays a central role in the mechanism of AFB1 toxicity in the heart,³² however, whether AFB1-induced oxidative stress is related to NLRP3 activation in the rat heart is not clear.

To investigate oxidative stress on the impact of the NLRP3 inflammasome, correlation analysis and a multiple linear regression model was used to identify the relationship between these variables. The results showed that oxidative stress parameters were positively correlated with NLRP3, ASC, caspase-1p20 and IL-1 β p17

expression. Furthermore, the antioxidant melatonin was applied to inhibit oxidative stress. Melatonin's ability to suppress NLRP3 inflammasome activation and decrease IL-1 β hypersecretion, due to its various antioxidant actions, has been fully documented in an LPS/ATP-induced murine microglia model.³³ In the present study, the addition of melatonin was shown to significantly attenuate ROS generation induced by high-dose AFB1. Notably, treatment with melatonin efficiently downregulated the degree of cardiac injury and serum LDH levels in high-dose AFB1-exposed rats. Proteomics analysis showed that increased expression of NLRP3 and other inflammasome-related proteins was partially reversed by melatonin; and these findings were confirmed by both immunohistochemistry and Western blot analysis. These results suggest that decreases in ROS levels induced by melatonin attenuated NLRP3 inflammasome activation and thus alleviated AFB1-induced cardiac injury. In addition, the results indicate that ROS-mediated NLRP3 inflammasome activation is the potential mechanism underlying the cardiac toxicity of AFB1.

Different downstream signals are shown to be selectively activated in different cell types upon the increased expression of inflammatory components.^{34,35} Increased IL-1 β secretion is observed in only cardiac fibroblasts and infiltrating inflammatory cells.^{36,37} NLRP3 inflammasome activation in cardiomyocytes leads to caspase-1-dependent cell death, presumably pyroptosis.³⁵ The authors' speculate that NLRP3-dependent cardiomyocyte pyroptosis might be an important mechanism in the cardiotoxicity of AFB1, and these conjectures should be experimentally verified in future studies.

A trigger is required to activate the NLRP3 inflammasome pathway, which is largely, but not exclusively, dependent on oxidative stress.^{38,39} Other factors in

addition to oxidative stress may regulate the expression of *NLRP3* in the hearts of AFB1-poisoned rats. *NLRP3* is not expressed constitutively in the heart but can be induced by activation of NF- κ B, for which sensors, such as Toll-like receptors (TLRs) and the IL-1 receptor, are required.^{31,40} Ochratoxin A has been found to enhance immunotoxicity through ROS-related TLR4 activation, and even activation of TLR4-driven (I κ B/NF- κ B) signalling exacerbates AFB1-promoted inflammation and tissue damage.⁴¹ Similar to this result, the present study found that AFB1 induced the activation of NF- κ B, however, the detailed mechanisms by which AFB1 activates NF- κ B signalling are not clear. NF- κ B is activated by oxidative stress, and its activation can be modulated by some antioxidants.^{42,43} Melatonin was revealed to significantly reduce expression and nuclear levels of NF- κ B in the present study, and the present authors believe that AFB1-induced NF- κ B activation might be tightly correlated with ROS, and melatonin suppresses NF- κ B signalling by inhibiting ROS production. Furthermore, as a key mediator of immunity, NF- κ B plays a critical role in the initiation of NLRP3 inflammasome activation, as NLRP3 itself is under the transcriptional control of the former.⁴⁰ The present data revealed a positive correlation between NF- κ B activation and *NLRP3* expression. Therefore, the priming step is likely to be initiated by ROS, thus activating the NF- κ B signalling pathway, which leads to an increase in the constitutive expression of AFB1-inducible NLRP3 and pro-IL-1 β . However, the specific signalling pathways require further verification.

In conclusion, the present study provides novel insight into the toxic action of AFB1 on rat hearts, which requires the NLRP3 inflammasome. AFB1 not only increases *NLRP3* expression, but also induces the activation of caspase-1 and the maturation

of IL-1 β . These effects seem to be mediated by oxidative stress and to be involved in the activation of NF- κ B. In addition, this study also confirmed that melatonin is a potential therapeutic agent for the management of myocardial damage caused by AFB1. Although the precise mechanisms underlying these effects were not thoroughly elucidated in the present study, the inhibitory activity of melatonin might be related to alleviation of oxidative stress and inhibition of NF- κ B activation in cardiac tissue, which in turn inhibits NLRP3 inflammasome activation. The results of the present study may be limited by the fact that there was no direct evidence of AFB1-induced NLRP3 inflammasome activation in myocardial injury at the cellular level, and the detailed mechanisms by which melatonin inhibits oxidative stress were not addressed.


Declaration of conflicting interest


The author(s) declared no potential conflicts of interest with respect to the research, authorship, and/or publication of this article.

Funding

The author(s) disclosed receipt of the following financial support for the research, authorship, and/or publication of this article: This work was funded by a grant from the Natural Science Foundation of Shandong Province (Grant No. ZR2017MH056).

ORCID iDs

Junhua Ge  <https://orcid.org/0000-0002-3119-6478>

Jian Li  <https://orcid.org/0000-0002-1924-8861>

References

1. Adepo JA, Manda P, Ngbe JV, et al. Study of aflatoxicosis reduction: effect of *Alchornea cordifolia* on biomarkers in an aflatoxin B1 exposed rats. *Drug Chem Toxicol* 2019; 42: 243–251.

2. Baan R, Grosse Y, Straif K, et al. A review of human carcinogens—Part F: chemical agents and related occupations. *Lancet Oncol* 2009; 10: 1143–1144.
3. Ge J, Yu H, Li J, et al. Assessment of aflatoxin B1 myocardial toxicity in rats: mitochondrial damage and cellular apoptosis in cardiomyocytes induced by aflatoxin B1. *J Int Med Res* 2017; 45: 1015–1023.
4. Yilmaz S, Kaya E, Karaca A, et al. Aflatoxin B1 induced renal and cardiac damage in rats: Protective effect of lycopene. *Res Vet Sci* 2018; 119: 268–275.
5. Abderrazak A, Syrovets T, Couchie D, et al. NLRP3 inflammasome: from a danger signal sensor to a regulatory node of oxidative stress and inflammatory diseases. *Redox Biol* 2015; 4: 296–307.
6. Martinon F, Burns K and Tschopp J. The inflammasome: a molecular platform triggering activation of inflammatory caspases and processing of proIL- β . *Mol Cell* 2002; 10: 417–426.
7. Swanson KV, Deng M and Ting JP. The NLRP3 inflammasome: molecular activation and regulation to therapeutics. *Nat Rev Immunol* 2019; 19: 477–489.
8. Toldo S and Abbate A. The NLRP3 inflammasome in acute myocardial infarction. *Nat Rev Cardiol* 2018; 15: 203–214.
9. Zhang LY, Zhan DL, Chen YY, et al. Aflatoxin B1 enhances pyroptosis of hepatocytes and activation of Kupffer cells to promote liver inflammatory injury via dephosphorylation of cyclooxygenase-2: an in vitro, ex vivo and in vivo study. *Arch Toxicol* 2019; 93: 3305–3320.
10. Carlomagno G, Minini M, Tilotta M, et al. From implantation to birth: insight into molecular melatonin functions. *Int J Mol Sci* 2018; 19: 2802.
11. Cheng L, Qin Y, Hu X, et al. Melatonin protects in vitro matured porcine oocytes from toxicity of Aflatoxin B1. *J Pineal Res* 2019; 66: e12543.
12. Reiter RJ, Guerrero JM, Escames G, et al. Prophylactic actions of melatonin in oxidative neurotoxicity. *Ann N Y Acad Sci* 1997; 825: 70–78.
13. Reiter RJ, Mayo JC, Tan DX, et al. Melatonin as an antioxidant: under promises but over delivers. *J Pineal Res* 2016; 61: 253–278.
14. Garcia JA, Volt H, Venegas C, et al. Disruption of the NF- κ B/NLRP3 connection by melatonin requires retinoid-related orphan receptor- α and blocks the septic response in mice. *FASEB J* 2015; 29: 3863–3875.
15. Bonomini F, Dos Santos M, Veronese FV, et al. NLRP3 inflammasome modulation by melatonin supplementation in chronic pristane-induced lupus nephritis. *Int J Mol Sci* 2019; 20: 3466.
16. Wang X, Bian Y, Zhang R, et al. Melatonin alleviates cigarette smoke-induced endothelial cell pyroptosis through inhibiting ROS/NLRP3 axis. *Biochem Biophys Res Commun* 2019; 519: 402–408.
17. Noda S. Histopathology of endomyocardial biopsies from patients with idiopathic cardiomyopathy; quantitative evaluation based on multivariate statistical analysis. *Jpn Circ J* 1980; 44: 95–116.
18. Sener G, Toklu H, Ercan F, et al. Protective effect of beta-glucan against oxidative organ injury in a rat model of sepsis. *Int Immunopharmacol* 2005; 5: 1387–1396.
19. Zhang J, Ma H, Yang L, et al. Silencing of the TROP2 gene suppresses proliferation and invasion of hepatocellular carcinoma HepG2 cells. *J Int Med Res* 2019; 47: 1319–1329.
20. Couto GK, Fernandes RO, Lacerda D, et al. Profile of pterostilbene-induced redox homeostasis modulation in cardiac myoblasts and heart tissue. *J Biosci* 2018; 43: 931–940.
21. Hu X, Li D, Wang J, et al. Melatonin inhibits endoplasmic reticulum stress-associated TXNIP/NLRP3 inflammasome activation in lipopolysaccharide-induced endometritis in mice. *Int Immunopharmacol* 2018; 64: 101–109.
22. Xiao L, Xu X, Zhang F, et al. The mitochondria-targeted antioxidant MitoQ ameliorated tubular injury mediated by mitophagy in diabetic kidney disease via Nrf2/PINK1. *Redox Biol* 2017; 11: 297–311.
23. Pollack A, Kontorovich AR, Fuster V, et al. Viral myocarditis—diagnosis, treatment

- options, and current controversies. *Nat Rev Cardiol* 2015; 12: 670–680.
24. Mirijello A, Tarli C, Vassallo GA, et al. Alcoholic cardiomyopathy: What is known and what is not known. *Eur J Intern Med* 2017; 43: 1–5.
 25. Wang W, Xu Z, Yu C, et al. Effects of aflatoxin B1 on mitochondrial respiration, ROS generation and apoptosis in broiler cardiomyocytes. *Anim Sci J* 2017; 88: 1561–1568.
 26. Karki R, Man SM, Malireddi RKS, et al. Concerted activation of the AIM2 and NLRP3 inflammasomes orchestrates host protection against *Aspergillus* infection. *Cell Host Microbe* 2015; 17: 357–368.
 27. Ketelut-Carneiro N, Silva GK, Rocha FA, et al. IL-18 triggered by the Nlrp3 inflammasome induces host innate resistance in a pulmonary model of fungal infection. *J Immunol* 2015; 194: 4507–4517.
 28. Jia C, Zhang J, Chen H, et al. Endothelial cell pyroptosis plays an important role in Kawasaki disease via HMGB1/RAGE/cathepsin B signaling pathway and NLRP3 inflammasome activation. *Cell Death Dis* 2019; 10: 778.
 29. Lamkanfi M and Dixit VM. Mechanisms and functions of inflammasomes. *Cell* 2014; 157: 1013–1022.
 30. He Y, Hara H and Nunez G. Mechanism and regulation of NLRP3 inflammasome activation. *Trends Biochem Sci* 2016; 41: 1012–1021.
 31. Zhao XJ, Yang YZ, Zheng YJ, et al. Magnesium isoglycyrrhizinate blocks fructose-induced hepatic NF- κ B/NLRP3 inflammasome activation and lipid metabolism disorder. *Eur J Pharmacol* 2017; 809: 141–150.
 32. Yilmaz S, Kaya E and Comakli S. Vitamin E (α tocopherol) attenuates toxicity and oxidative stress induced by aflatoxin in rats. *Adv Clin Exp Med* 2017; 26: 907–917.
 33. Arioz BI, Tastan B, Tarakcioglu E, et al. Melatonin attenuates LPS-induced acute depressive-like behaviors and microglial NLRP3 inflammasome activation through the SIRT1/Nrf2 pathway. *Front Immunol* 2019; 10: 1511.
 34. Takahashi M. Cell-specific roles of NLRP3 inflammasome in myocardial infarction. *J Cardiovasc Pharmacol* 2019; 74: 188–193.
 35. Mezzaroma E, Toldo S, Farkas D, et al. The inflammasome promotes adverse cardiac remodeling following acute myocardial infarction in the mouse. *Proc Natl Acad Sci U S A* 2011; 108: 19725–19730.
 36. Sandanger Ø, Ranheim T, Vinge LE, et al. The NLRP3 inflammasome is up-regulated in cardiac fibroblasts and mediates myocardial ischaemia-reperfusion injury. *Cardiovasc Res* 2013; 99: 164–174.
 37. Takahashi M. NLRP3 Inflammasome as a novel player in myocardial infarction. *Int Heart J* 2014; 55: 101–105.
 38. Jo EK, Kim JK, Shin DM, et al. Molecular mechanisms regulating NLRP3 inflammasome activation. *Cell Mol Immunol* 2016; 13: 148–159.
 39. Tschopp J and Schroder K. NLRP3 inflammasome activation: The convergence of multiple signalling pathways on ROS production? *Nat Rev Immunol* 2010; 10: 210–215.
 40. Toldo S, Mezzaroma E, McGeough MD, et al. Independent roles of the priming and the triggering of the NLRP3 inflammasome in the heart. *Cardiovasc Res* 2015; 105: 203–212.
 41. Hou L, Gan F, Zhou X, et al. Immunotoxicity of ochratoxin A and aflatoxin B1 in combination is associated with the nuclear factor kappa B signaling pathway in 3D4/21 cells. *Chemosphere* 2018; 199: 718–727.
 42. Jeong WS, Kim IW, Hu R, et al. Modulatory properties of various natural chemopreventive agents on the activation of NF- κ B signaling pathway. *Pharm Res* 2004; 21: 661–670.
 43. Ma Q, Li Y, Fan Y, et al. Molecular mechanisms of lipoic acid protection against aflatoxin B₁-induced liver oxidative damage and inflammatory responses in broilers. *Toxins (Basel)* 2015; 7: 5435–5447.